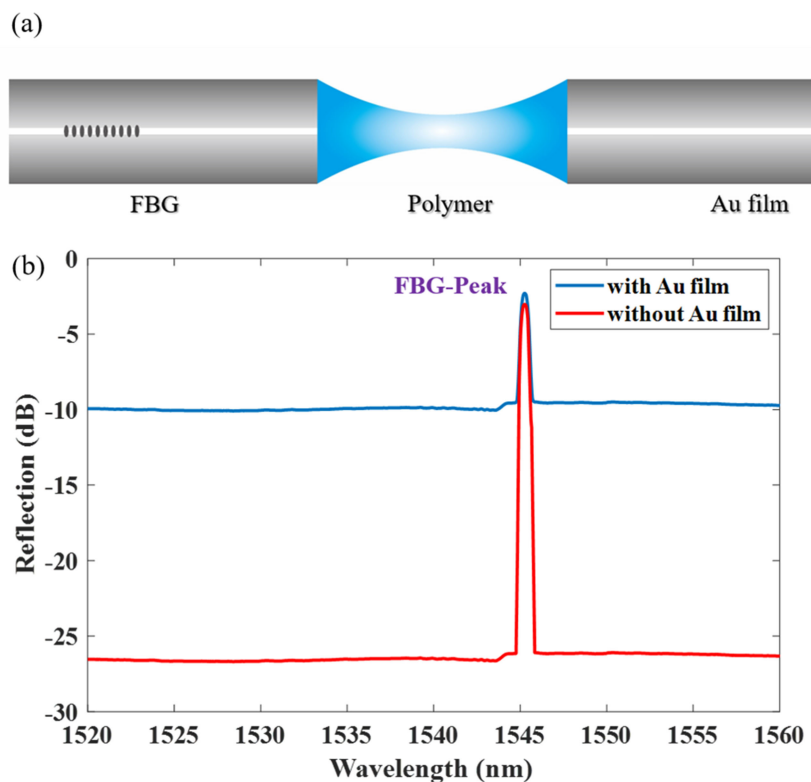


Tapered Polymer Fiber Inclinometers

Volume 12, Number 3, June 2020

Cheng-Ling Lee
Rui-Cheng Zeng
Chun-Ren Yang
Chi-Feng Lin
Chao-Tsung Ma
Wen-Fung Liu



DOI: 10.1109/JPHOT.2020.2974796

Tapered Polymer Fiber Inclinometers

Cheng-Ling Lee¹, Rui-Cheng Zeng,¹ Chun-Ren Yang,¹
Chi-Feng Lin,¹ Chao-Tsung Ma², and Wen-Fung Liu³

¹Department of Electro-Optical Engineering, National United University, Miaoli City 36003, Taiwan

²Department of Electrical Engineering, National United University, Miaoli City 36003, Taiwan

³Department of Electrical Engineering, Feng-Chia University, Taichung 40724, Taiwan

DOI:10.1109/JPHOT.2020.2974796

This work is licensed under a Creative Commons Attribution 4.0 License. For more information, see <http://creativecommons.org/licenses/by/4.0/>

Manuscript received January 20, 2020; revised February 10, 2020; accepted February 13, 2020. Date of publication February 18, 2020; date of current version June 26, 2020. This work was supported by the Ministry of Science and Technology of Taiwan, MOST 107-2221-E-239-017 and MOST 108-2221-E-239-020. Corresponding author: Cheng-Ling Lee (e-mail: cherry@nuu.edu.tw).

Abstract: This work proposes a novel, highly sensitive, and simple structure based on a tapered polymer as a tilt fiber sensor to sensitively measure tilt angles (θ). The fiber-optic tilt sensor consists of a tapered polymer and single-mode fibers (SMF), into which the tapered polymer to generate a bent in the sensor that is strongly correlated with θ . The used tapered polymer in the tilt sensing is the temperature (T) insensitive. It is further combined with a general fiber Bragg grating (FBG) as a temperature indicator for achieving simultaneous measurement of inclination (θ) and ambient T. The endface of the fiber is coated with a gold film to increase the light reflectivity and improve the measurement range. Experimental results show that when the sensor tilts, the reflective optical power changes significantly with high sensitivity, and the peak wavelength of FBG shifts when T varies. Both parameters can be measured simultaneously with good discrimination. An average tilt angle sensitivity of approximately 4.23 dB/deg. and a high resolution of 0.009 deg. are achieved in a θ variation from -6 to $+6$ deg. Simulations were performed and the numerical results were in *good agreement* with the experimental measurement.

Index Terms: Fiber Bragg grating (FBG), fiber optics inclination sensor, taper-shaped polymer, tilt fiber sensor.

1. Introduction

With the number and size of civil engineering projects being constructed continuing to increase, such as high-rise buildings, bridges, and dams, the use of inclinometers to detect variations in the tilt angle (θ) within structures is significant and urgent. Accurate tilt sensors with high sensitivity are one of the most common sensors for determining the inclination of buildings. Other applications, for example, measuring landslide and ground movements and monitoring the inclination of bridges and structure of industrial machines, are included. Thus, a cost-effective, simple-structured, sensitive, and extremely accurate tilt sensor that meets engineering requirements must be developed. Compared to traditional electrical tilt sensors, fiber-optic sensors have many advantages, including immunity to electromagnetic interferences, remote sensing capability, high sensitivity and potential small size; as such, several tilt fiber sensors have been proposed in recent years [1]–[13]. Among fiber-optic tilt sensors, those whose fibers have a tapered structure are generally regarded as having a more sensitive configuration [1]–[6], [10]–[13]. In 2011, a compact inclinometer sensor based on a fiber-taper Michelson interferometer was presented to demonstrate its effectiveness

TABLE 1
Comparison of Material Properties [17]

Materials	NOA61	NOA65	NOA87	Optical fiber
Modulus of Elasticity (PSI)	150,000	20,000	209,700	11,284,00
Elongation at Failure	38%	80%	13%	0.8%

in sensing θ [1]. Next, an optical fiber interferometer based on an abrupt fiber taper, cascading peanut-shaped fiber was proposed for tilt angle measurements with high sensitivity in the range of 0–6.66 deg. [2]. Similarly, a tilt fiber sensor consisting of a microtaper fiber incorporating an air-gap microcavity for bending angles from –4 to 4 deg. was presented [3]. A taper section and lateral-offset fusion splicing fiber was proposed to achieve fiber-optic interferometric-type tilt angle sensors with high sensitivity from –5 to 5 deg. In the tapered region, several cladding modes were excited and then core-higher cladding mode interference occurred at the lead-out fiber when the lateral offset was controlled [4]. Fiber Mach–Zehnder interferometers based on the connection of two fiber tapers were proposed to investigate the extremely high sensitivity of interferometric-type tilt fiber sensors [5], [6]. The most well-known fiber tilt sensors are based on fiber Bragg gratings (FBGs), which have numerous benefits in terms of reliability and distributed capability [7], [9]. Thus, fiber tapers that have been further incorporated with designed FBGs that can form smart and functional tilt fiber sensors for the simultaneous measurement of tilt angle (θ) and temperature (T) [10]–[12] and the vector inclination sensing [13].

In this study, we propose a novel tapered polymer fiber tilt sensor (TPFTS) with simple structure to sensitively measure θ . This is for the first time the polymer materials of NOA series were utilized in the fibers to be found the good bonding with fiber as well as high sensitivity of tilt angle variation [14]. The proposed TPFTS is based on a type of optical adhesive, NOA65 ultraviolet (UV)-cured polymer with good elongation and is more elastic than conventional fiber taper based tilt sensors [15]. The structure of TPFTS is also temperature insensitive and can be further combined with a general FBG as a temperature indicator for the simultaneous measurement of inclination and ambient T. With the presented configuration, the proposed sensor can measure θ and T simultaneously with high sensitivity. The taper structure made of polymer is more sensitive in tilt sensing than the fiber taper made by SMF because the former is coreless with more flexibility. Then, a gold (Au) thin film always used in the surface plasmon resonance (SPR) of biosensors [15], [16] is coated on the endface of the fiber to increase the light reflectivity and improve the measurement range. Experimental results show that the proposed tapered polymer sensing element responds well to tilt. An average tilt angle sensitivity of approximately 4.23 dB/deg. and a high resolution of 0.009 deg. are achieved in a θ variation from –6 to +6 deg. The results also reveal that the highest sensitivity of 5.76 dB/deg. at ± 2.5 deg. by the sensor have been presented.

2. Sensor Fabrication and Principle

In this experiment, we selected NOA65 polymer to make the unique and novel fiber sensing structure. Table 1 lists the comparison of physical/mechanical characteristics of several materials, including optical fiber. The properties of the fiber and polymer materials are quite different from the values shown in the Table 1. The low modulus of elasticity of NOA65 means the polymer is more flexible and easier to bent than other materials. Large elongation at failure indicates the high stretch capability of the NOA65. Thus, on the basis of data in the list, NOA65 is the best candidate for tilt angle measurement.

The taper-shaped polymer was simply fabricated with the assistance of three-axis translation stages at good alignment conditions. During the fabrication process, the proposed sensor was

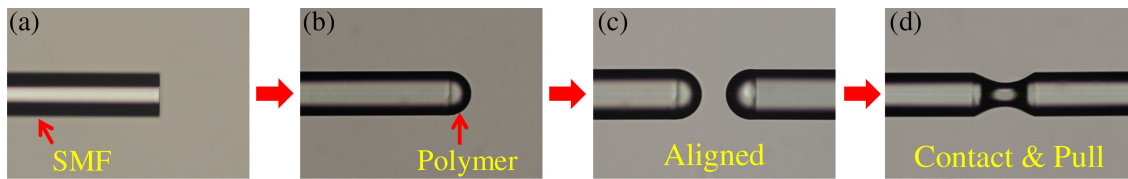


Fig. 1. Fabrication process of the taper-shaped polymer.

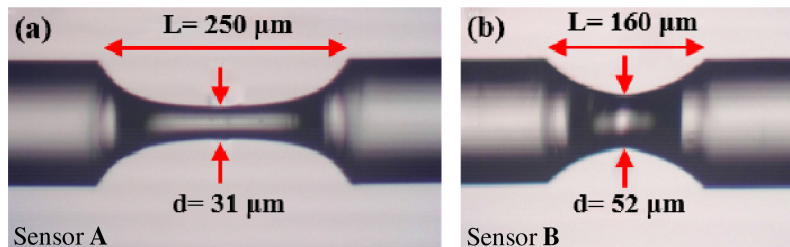


Fig. 2. Microphotographs of different structures of the taper-shaped polymer, (a) sensor A with $L/d = 250 \mu\text{m}/31 \mu\text{m}$, and (b) sensor B with $L/d = 160 \mu\text{m}/52 \mu\text{m}$.

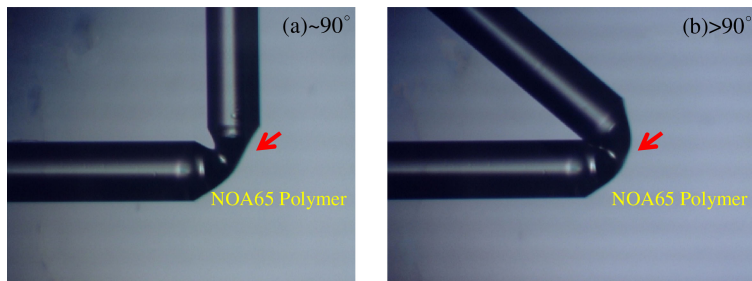


Fig. 3. Micrograph of the taper-shaped polymer bent at high angles of (a) 90° and (b) $>90^\circ$.

monitored by a CCD microscope. As can be seen in Fig. 1, step (a): the endface of the SMF was cleaved flat and placed on the three-axis translation stage. In steps (b) and (c), the monitored translation stages were used to attach the thick film of NOA65 onto the endface of the SMFs. In step (d), the two endfaces of the polymer were arranged into close, aligned contact and then pulled into the desired taper shape. Finally, the polymer was cured by exposure to UV light to form a solid polymer structure. Thus, the structure of the taper-shaped polymer is a cylinder with a thinnest waist in the middle and both endfaces matched the size of fibers. Different structures of the taper-shaped polymer can be accomplished by using this fabrication process, as shown in microphotographs of Fig. 2. The figure illustrates the structures of the taper-shaped polymer, which can have tapered region $L = 250 \mu\text{m}$ and $160 \mu\text{m}$ long and thinnest waist diameter $d = 31 \mu\text{m}$ and $52 \mu\text{m}$ for sensor A and sensor B, as shown in Fig. 2(a) and 2(b), respectively.

In Fig. 3, the main bending and stretching part of the component is the polymer whose modulus of elasticity can reveal that the produced tapered polymer will be more flexible than the tapered fiber made of SMF and will have higher sensitivity in tilt sensing. Fig. 3 shows that not only can the above characteristics be confirmed, but the tapered polymer made of NOA65 can be bent to a high angle without breaking easily.

To ensure the sensor has maximum light reflectivity, the endface of the fiber was coated with Au thin film to increase light reflectivity and improve measurement range. The results are shown in Fig. 4. Fig. 4(a) plots the schematic diagram of the proposed taper-shaped polymer-fiber-coated

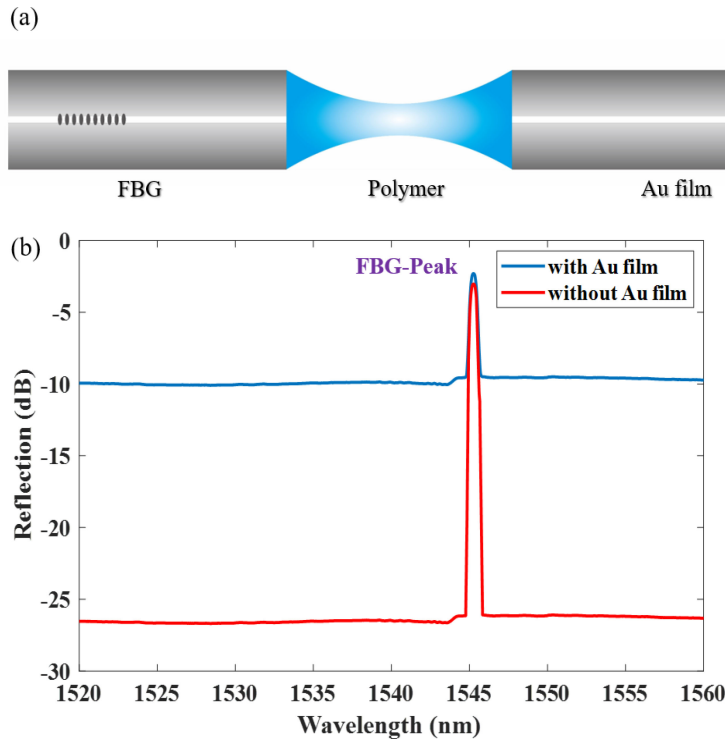


Fig. 4. (a) Schematic diagram of the proposed taper-shaped polymer-fiber-coated Au thin film combined with an FBG. (b) Measured reflection spectra with Au thin film coating.

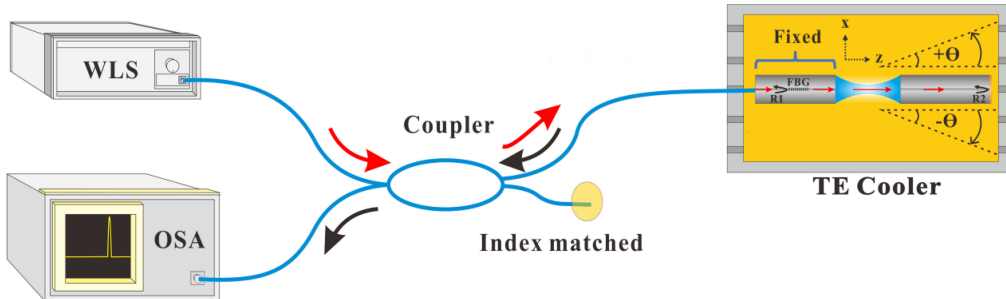


Fig. 5. Experimental setup and operating principle for simultaneously measuring the inclination and ambient T.

Au thin film and further combined with an FBG as temperature indicator. The measured reflection spectra of the sensor with Au thin film coating are shown in Fig. 4(b). As shown in Fig. 4(b), the device with Au film has much higher reflectivity over 17 dB than that of the device without Au film within the sideband. Thus, Au coating can increase light reflectivity to improve the measurement range of θ .

Experimental setup and operation principle of the proposed tilt sensor is shown in Fig. 5. The wideband light source (WLS) propagates from the FBG side. When the light reaches the FBG, it will produce the first reflected peak (R_1) at Bragg wavelength. However, for the remaining light transmitted in the taper-shaped polymer section, some of the light will leak out into the surrounding. Finally, the light will reach the Au film with high reflection of R_2 . When the taper-shaped polymer is bent due to the tilt situation, light propagates from the taper-shaped polymer, and transmission into the lead-out fiber will substantially decrease with deviation from the center of fiber. Meanwhile, the reflected peak in FBG would almost not be changed by the variation of θ but responses to various

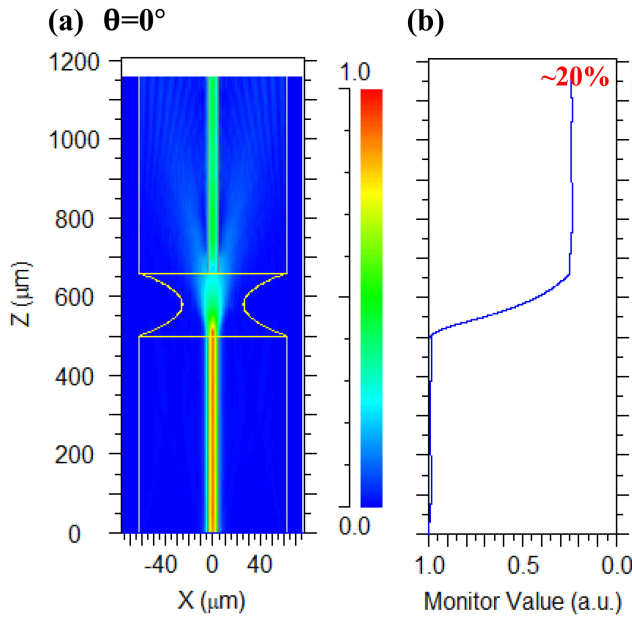


Fig. 6. FDBPM simulation results of (a) mode field distribution of light and (b) normalized intensity at optical axis $X = 0$ propagating along z axis inside the sensor at tilt angle of $\theta = 0^\circ$.

temperatures. It should be noted that to prevent misalignment between the center axes of polymer taper and SMF a tiny hard strip was attached to the sensor for achieving correct tilt angles.

To understand more optical characteristics of the proposed polymer taper, it was performed simulation work first. The intensity of light that propagates along the z axis inside the tapered-polymer fiber can be calculated by using the numerical finite difference beam propagation method (FDBPM) algorithm (Rsoft Beam PROP). Wavelength of the input light is set to be $\lambda = 1550 \text{ nm}$. The polymer taper of sensor B with $L = 160 \mu\text{m}$, $d = 52 \mu\text{m}$ and refractive index: $n = 1.524$ at $\lambda = 1550 \text{ nm}$ was connected with two single mode fibers. The FDBPM simulation results show that the normalized intensity of light strongly decays when the sensor tilts, as shown in Figs. 6–8. The Figs. 6(a) and 7(a) show the simulation results of mode field distribution of light propagating through the proposed polymer fiber at tilt angles of 0° and 5° , respectively. Optical mode field expands and leaky out through the polymer tapered region with the light intensity of about 20% and 4% remained to the output SMFs for $\theta = 0^\circ$ and $\theta = 5^\circ$, as respectively plotted in Figs. 6(b) and 7(b). Here, the normalized intensities shown in the Figs. 6(b) and 7(b) are monitored at optical axis $X = 0$ propagating along z axis inside the fibers. Fig. 8 investigates the optical power of light traveling through the tapered-polymer is highly related to the tilt angles. As can be seen that the optical light was suffered strong loss when propagating through the polymer tapered region. A higher tilt angle can result a sharper transition of power decay in the polymer taper region of the fiber sensor.

3. Experimental Results and Discussion

The fabrication and sensing principle of the sensor have been described above. In this section, we study the feasibility of the proposed method and sensing construction. The light from a wideband light source (WLS) propagates into the device, and the combined reflection spectra of the FBG and tilt sensor are obtained using an optical spectrum analyzer (OSA). Here, a thermoelectric cooler is used to control the surrounding T of the tapered polymer tilt fiber sensor.

The tilt is employed on the sensor at a fixed T for the positive and negative tilt angles and its optical responses are shown in Fig. 9(a) and (b), respectively. Almost the same spectral responses

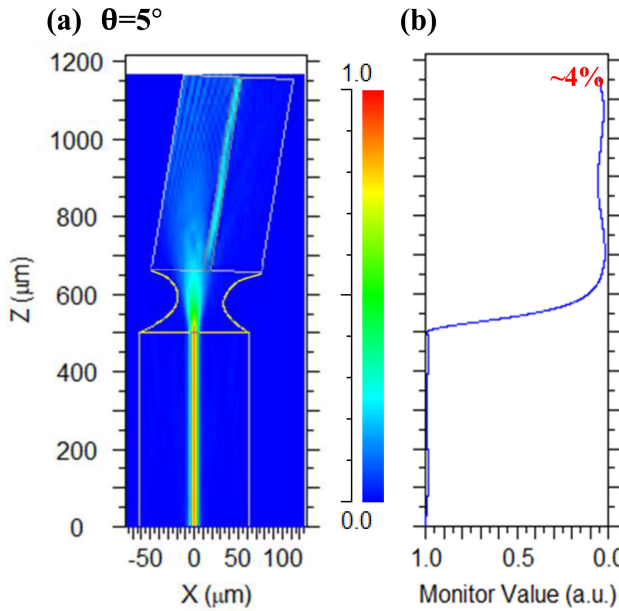


Fig. 7. FDBPM simulation results of (a) mode field distribution of light and (b) normalized intensity at optical axis $X = 0$ propagating along z axis inside the sensor at tilt angle of $\theta = 5^\circ$.

indicate the tapered polymer structure has central symmetry. When the sensor tilts, the optical power of reflection in the sideband strongly decays, but due to the fixed T , the wavelength peak of FBG almost does not shift. The experimental results reveal that the sensor is tilt symmetrical to present similar optical responses to the positive and negative angles. Moreover, the reflection in the sideband no longer changed when θ is over ± 12 deg.

Fig. 9(c) shows the reflection variation of sensor **A** and **B** at 1550 nm wavelength as the θ changes from -12 to 12 deg. with a step of 1 deg. When the sensors bend because of the tilt, the sideband reflection strongly decays at a small θ . However, at high angles, the reflection will gradually smoothen and will not vary because the bending action will have almost leaked out the signal light. The relationship between variation of normalized reflection (ΔR) and θ can be simply expressed as follows:

$$\Delta R = p e^{-q\theta^2} \quad (1)$$

In Eq. (1), p and q are the constants of the exponential fitting curve that are correlated with the tilt sensor sensitivity and the sensitivity properties of two structures are shown in Table 2, respectively. The value of p can equivalently represent the total response during the whole measurement range. The q denotes the attenuation coefficient of the Gaussian curve in Eq. (1).

From the Eq. (1), θ is easily determined as follows:

$$\theta = \pm \sqrt{\frac{1}{q} \ln \left(\frac{\Delta R}{p} \right)} \quad (2)$$

on the basis of Eq. (2), the θ can be estimated when the values of ΔR are measured. Owing to the symmetry of the polymer's tapered shape, similar optical responses are presented to the $+\theta$ and $-\theta$ tilt states.

Equation (1) can be differentiated to obtain the sensitivity with respect to the θ , as defined below:

$$S = \left| \frac{d(\Delta R)}{d\theta} \right| \quad (3)$$

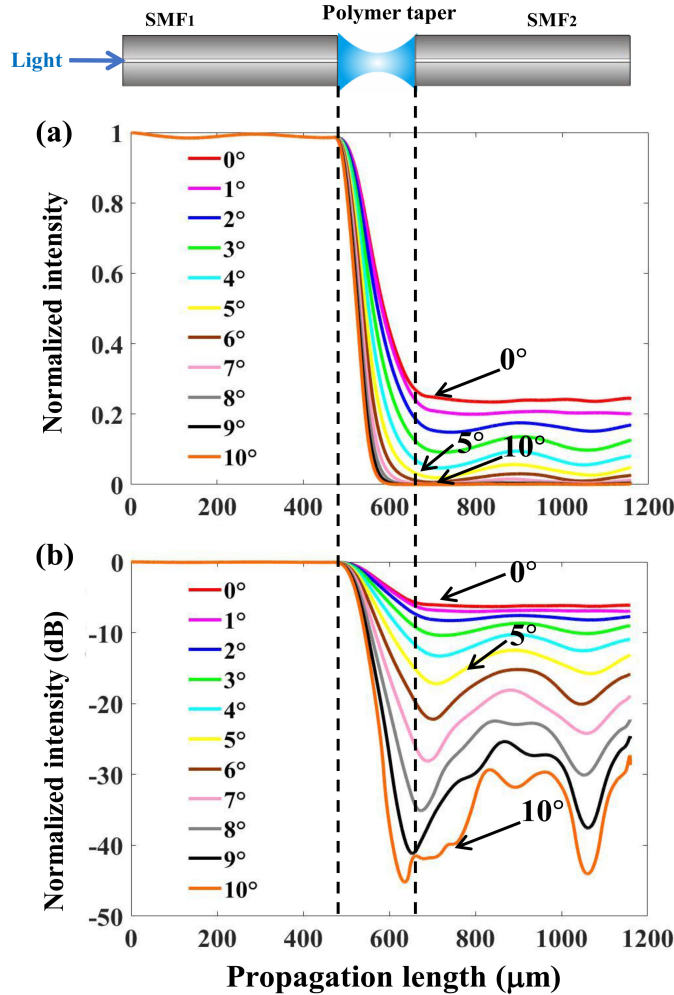


Fig. 8. Simulation results of normalized intensity at optical axis $X = 0$ propagating along z axis with different tilt angles for (a) linear scales and (b) dB scales.

When the developed sensing structures of sensor **A** and **B** are used (as shown in Fig. 2), tilt responses and sensitivities for the variation from -12 to $+12$ deg. are obtained and shown in Fig. 9(c) and (d), respectively. Sensor **A** with thinner taper seems to be more sensitive than that of sensor **B**. However, the tilt measurement range is relatively small for sensor **A**. Insets of the Fig. 9(c) shows the average tilt angle sensitivities having approximately 4.23 dB/deg. and 2.87 dB/deg. for the range of -6 to $+6$ deg. with sensor **A** and **B**, respectively. Therefore, given the 0.04 dB resolution of the used OSA, the average resolution of a θ variation from -6 to $+6$ deg. are calculated as 0.009 deg. and 0.014 deg. for sensor **A** and sensor **B**, respectively. The measurement ranges of sensor **A** and sensor **B** with -10 to $+10$ deg. and -12 to $+12$ deg., respectively are also presented in Fig. 9(d). The results in Fig. 9(d) also reveal that the highest sensitivities of 5.76 dB/deg. at ± 2.5 deg. and 3.21 dB/deg. at ± 3.2 deg. for sensor **A** and sensor **B**, respectively are achieved. The sensing results in Fig. 9 can also be evaluated by monitoring the reflection optical power at a certain wavelength. It can be seen that experimental results are in good agreement with the simulation results to investigate the effectiveness.

Fig. 10 demonstrates the recorded stability of a 160-minute measurement at the wavelength of 1550 nm. Figs. 11(a) and (b) display the temperature responses of the sensor when it is at a fixed θ of 0 deg. Fig. 11(a) shows the wavelength shift of FBG at temperatures of 30 °C– 90 °C. The peak of FBG is red-shifted as the T increased. However, the sideband energy does not decay, remaining

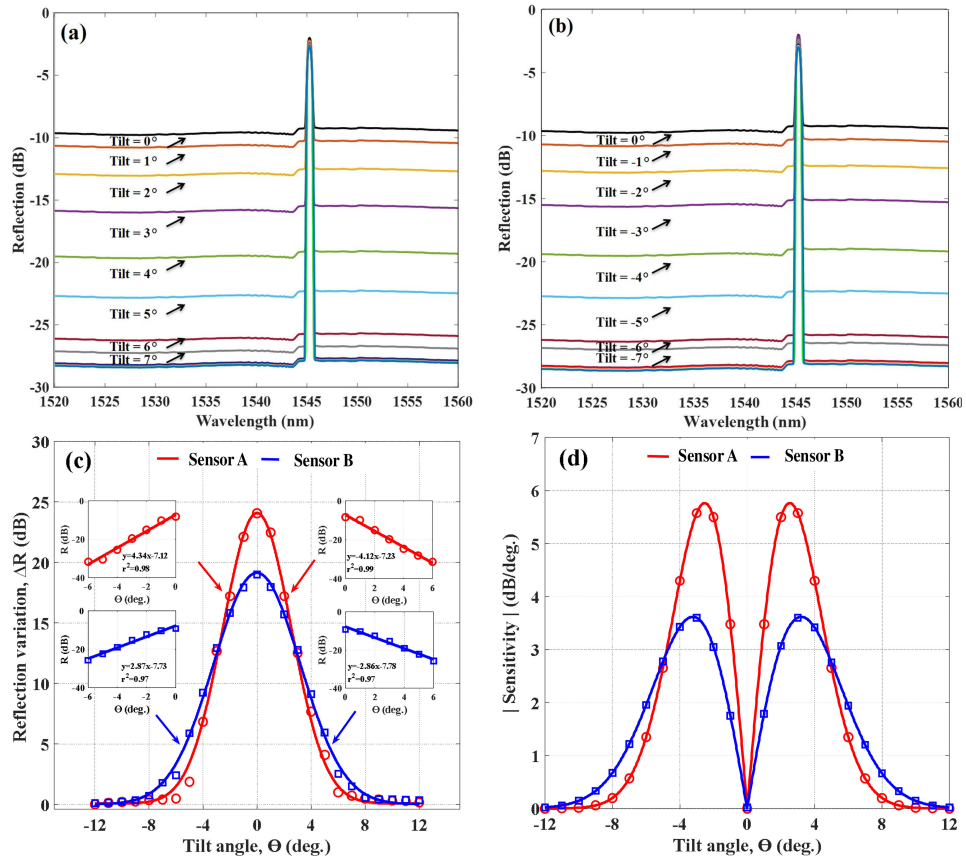


Fig. 9. Variations of reflection spectra of sensor B at tilt angles of (a) positive and (b) negative. (c) Responses of reflection variation to θ at wavelength of 1550 nm by sensor A and B. (d) Tilt-related sensitivity of the tapered polymer sensors.

TABLE 2
Comparison of Sensitivities of the Tapered Polymers With Different Structure

Sensor	Structure (μm) Length/Waist	Fitted Gaussian Equation	R-square
Sensor A	250/31	$\Delta R = 24e^{-0.28\theta^2}$	0.9962
Sensor B	160/52	$\Delta R = 19e^{-0.22\theta^2}$	0.9974

almost unchanged because the tapered polymer only affected by the variation of θ to show the proposed TPFTS is temperature insensitive. Furthermore, due to the fact that the thermo-optic coefficient (TOC) of the used polymer is about -2×10^{-4} (1/°C), the refractive index change is very small within the range of 30 °C to 90 °C. Fig. 11(b) shows the measured sensitivity of T for the wavelength shifts of the measured spectrum's FBG peak (blue line) and sideband energy of the tapered polymer (red line) at various temperatures. The results show the temperature indicator FBG has a linear response to T. The wavelength resolution of OSA is 0.01 nm, and so the temperature resolution is about 0.75 °C when using the sensing configuration.

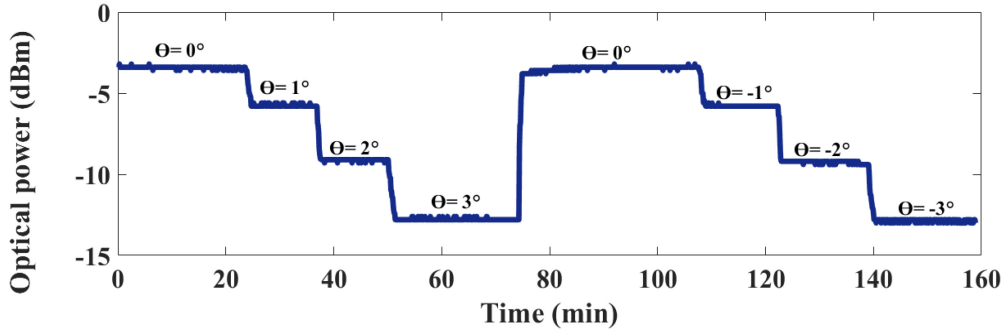


Fig. 10. Laser power measured by a photo-detector in different tilt angles for long time testing.

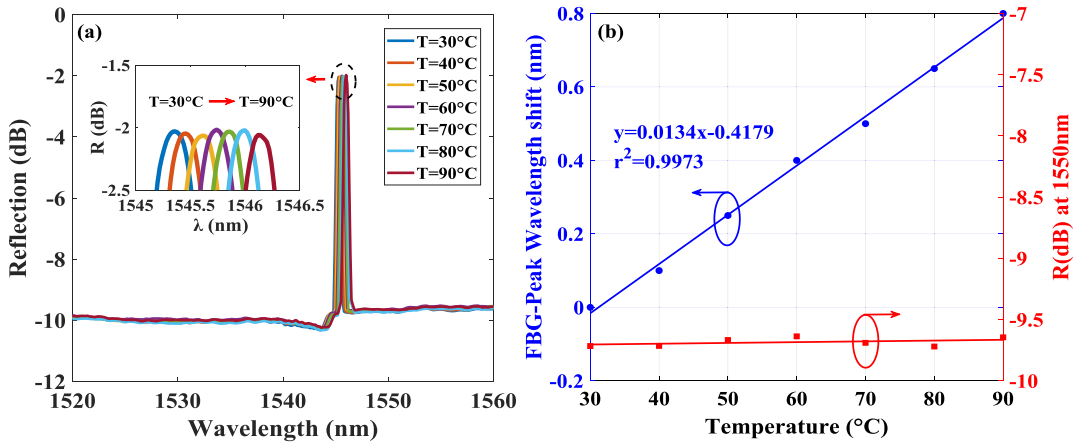


Fig. 11. (a) Temperature response of the sensor from 30 °C to 90 °C at a fixed θ . (b) Spectral sensitivities of the FBG peak and the tapered polymer at various T.

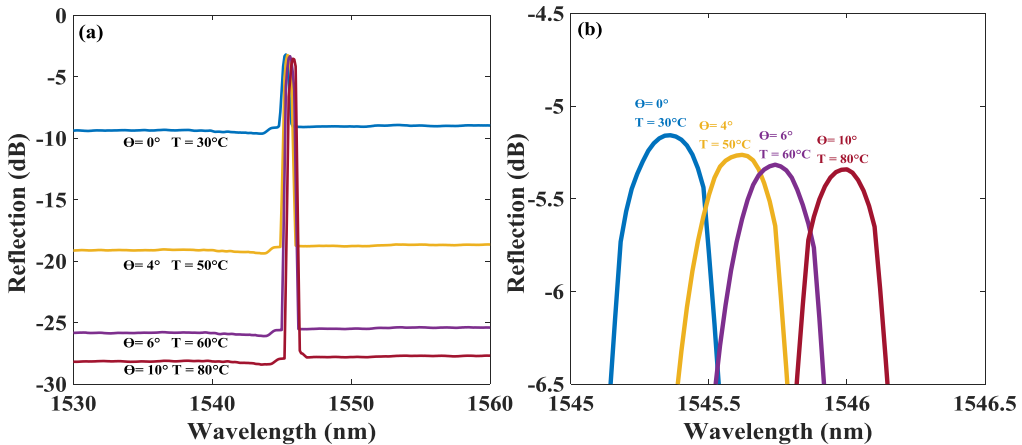


Fig. 12. (a) Reflection spectra of the sensor with different T and tilt conditions. (b) Details of peak wavelength shifts of the FBG.

Fig. 12(a) presents the optical spectra of the sensor for many cases of simultaneously changing θ and T. Fig. 12(b) shows the details of peak wavelength shifts of the FBG with T varied. Experimental results show that the peak wavelength linearly redshifts the FBG with the rise in T. Note that the tapered polymer is particularly sensitive to tilt, and FBG is only sensitive to T in the proposed

sensing configuration. Therefore, the sensor can measure tilt and T simultaneously with high sensitivity and good discrimination. For practical application, the fiber sensor needs to be further packaged with available materials of microtubes or would be skillfully integrated into the building or bridge tailored to critical application of inclinations.

4. Conclusion

This work proposes a simple fiber-optic tilt angle sensor based on a taper-shaped polymer combined with an FBG as a tilt fiber sensor that can measure T simultaneously. The taper-shaped polymer is insensitive to T and produces a bent that is much strongly correlated with θ . On the other hand, the FBG in the structure is nonreactive to θ but sensitive to T. Experimental results demonstrate that the optical power is changed when the sensor is tilted. Therefore, θ can be determined from the optical power. An average tilt response is obtained with sensitivity of 4.23 dB/deg. when θ is varied from -6 to $+6$ deg. by using the developed tapered polymer with $L = 250 \mu\text{m}$ and $d = 31 \mu\text{m}$. In addition, based on the peak wavelength shifts of FBG when T varies, the resolutions for T and θ of the proposed sensor are 0.75°C and 0.009 deg., respectively. Simulation results has demonstrated a good agreement with the experimental measurement in the study. The advantages of the proposed sensor are its simplicity, ease of fabrication, long-distance sensing, and high sensitivity. Future research on the presented solution may focus on improving the sensor to achieve better parameters and practical applications, such as directional performance and combined with real objects.

References

- [1] L. M. N. Amaral, O. Frazao, J. L. Santos, and A. B. L. Ribeiro, "Fiber-optic inclinometer based on taper michelson interferometer," *IEEE Sensors J.*, vol. 11, no. 9, pp. 1811–1814, Sep. 2011.
- [2] H. Gong, Z. Qian, and X. Yang, "Optical fiber inclinometer based on a fiber taper cascading a peanut-shape structure," *IEEE Sensors J.*, vol. 15, no. 7, pp. 3917–3920, Jul. 2015.
- [3] Z. Feng, T. Gang, M. Hu, X. Qiao, N. Liu, and Q. Rong, "A fiber inclinometer using a fiber microtaper with an air-gap microcavity fiber interferometer," *Opt. Commun.*, vol. 364, pp. 134–138, 2016.
- [4] M. Deng, Y. Zhao, F.-Y. Yin, and T. Zhu, "Interferometric fiber-optic tilt sensor exploiting taper and lateral-offset fusing splicing," *IEEE Photon. Technol. Lett.*, vol. 28, no. 20, pp. 2225–2228, Oct. 2016.
- [5] C. L. Lee, W. C. Shih, J. M. Hsu, and J. S. Horng, "Asymmetrical dual tapered fiber mach-zehnder interferometer for fiber optic directional tilt sensor," *Opt. Exp.*, vol. 22, no. 20, pp. 24646–24654, 2014.
- [6] C. L. Zhao, R. Wang, Y. Zhou, L. Niu, and H. Gong, "Angle sensor based on two cascading abrupt-tapers modal interferometer in single mode fiber," *Optik - Int. J. Light Electron Opt.*, vol. 132, pp. 236–242, 2017.
- [7] X. Dong, C. Zhan, K. Hu, P. Shum, and C. C. Chan, "Temperature-insensitive tilt sensor with strain-chirped fiber bragg gratings," *IEEE Photon. Technol. Lett.*, vol. 17, no. 11, pp. 2394–2396, Nov. 2005.
- [8] H. Y. Chang, Y. C. Chang, and W. F. Liu, "A highly sensitive two-dimensional inclinometer based on two etched chirped-fiber-grating arrays," *Sensors*, vol. 17, 2017, Art. no. 2922.
- [9] H. Y. Au, S. K. Khijwania, H. Y. Fu, W. H. Chung, and H. Y. Tam, "Temperature-insensitive fiber bragg grating based tilt sensor with large dynamic range," *J. Lightw. Technol.*, vol. 29, no. 11, pp. 1714–1720, 2011.
- [10] T. Osuh, K. Markowski, and K. Jedrzejewski, "Temperature independent tapered fiber bragg grating-based inclinometer," *IEEE Photon. Technol. Lett.*, vol. 27, no. 21, pp. 2312–2215, Nov. 2015.
- [11] C. Guo, D. Chen, C. Shen, Y. Lu, and H. Liu, "Optical inclinometer based on a tilted fiber bragg grating with a fused taper," *Opt. Fiber Technol.*, vol. 24, pp. 30–33, 2015.
- [12] T. Osuh, K. Markowski, A. Manujlo, and K. Jedrzejewski, "Coupling independent fiber optic tilt and temperature sensor based on chirped tapered fiber Bragg grating in double-pass configuration," *Sensors Actuators A Physical*, vol. 252, pp. 76–81, 2016.
- [13] L. Y. Shao and J. Albert, "Compact fiber-optic vector inclinometer," *Opt. Lett.*, vol. 35, no. 7, pp. 1034–1036, 2010.
- [14] J. Y. Guo, M. S. Wu, C. L. Lee, W. F. Liu, and C. F. Lin, "Simultaneous measurement of tilt angle and temperature based on a taper-shaped polymer incorporating a fiber bragg grating," in *Proc. Conf. Lasers Electro-Opt. Pacific Rim*, 2018, pp. 1–2.
- [15] M. S. Islam *et al.*, "A hi-bi ultra-sensitive surface plasmon resonance fiber sensor," *IEEE Access*, vol. 7, pp. 79085–79094, 2019.
- [16] M. S. Islam, C. M. R. Islam, J. Sultana, A. Dinovitser, B. W. H., and D. Abbott, "Exposed-core localized surface plasmon resonance biosensor," *J. Opt. Soc. Amer. B.*, vol. 36, no. 8, pp. 2306–2311, 2019.
- [17] Polymer material from Norland Products, Inc. [Online]. Available: <https://www.norlandprod.com/adhchart.html>